Activation of oestrogen receptor induces a novel form of LTP at hippocampal temporoammonic-CA1 synapses

Clements, Leigh; Harvey, Jenni

Published in:
British Journal of Pharmacology

DOI:
10.1111/bph.14880

Publication date:
2020

Document Version
Peer reviewed version

Harvey Jenni (Orcid ID: 0000-0002-9858-001X)

Activation of estrogen receptor α induces a novel form of long-term potentiation at hippocampal temporoammonic-CA1 synapses.

Leigh Clements, Jenni Harvey*

Division of Systems Medicine, Ninewells Hospital and Medical School, University of Dundee, DD1 9SY.

* Corresponding author: Dr Jenni Harvey,

Division of Systems Medicine,

Ninewells Hospital and Medical School,

University of Dundee,

DD1 9SY.

Tel: +44 1382 383359

Email: j.z.harvey@dundee.ac.uk

Running Title: ERα-induced LTP at TA-CA1 synapses

Word count (excluding abstract, methods, figure legends and references): 3998

Acknowledgements: This work was supported by grants from The Cunningham Trust and Alzheimer's Research UK Scotland Network Centre

This is the peer reviewed version of the following article: Clements, L. & Harvey, J. "Activation of estrogen receptor α induces a novel form of long‐term potentiation at hippocampal temporoammonic‐CA1 synapses", *British Journal of Pharmacology* (2019), which has been published in final form at https://doi.org/10.1111/bph.14880. This article may be used for non-commercial purposes in accordance with Wiley Terms and Conditions for Self-Archiving.

Abstract.

Background:

17β estradiol (E2) rapidly regulates excitatory synaptic transmission at the classical Schaffer collateral (SC) input to hippocampal CA1 neurons. However, the impact of E2 on excitatory synaptic transmission at the distinct temporoammonic (TA) input to CA1 neurons, and the estrogen receptors involved, are less clear.

Experimental Approach:

Extracellular recordings were used to monitor excitatory synaptic transmission in hippocampal slices from juvenile male (P11-24) Sprague Dawley rats. Immunocytochemistry combined with confocal microscopy was used to monitor the surface expression of the AMPA receptor (AMPAR) subunit, GluA1 in hippocampal neurons cultured from neonatal (P0-3) rats.

Results:

Here we show that E2 induces a novel form of LTP at TA-CA1 synapses; an effect mirrored by the ERα agonist, PPT and blocked by an ERα antagonist. ERα-induced LTP is NMDA receptor (NMDAR)-dependent and involves a postsynaptic expression mechanism that requires PI 3-kinase signalling and synaptic insertion of GluA2-lacking AMPA receptors. ERα-induced LTP has overlapping expression mechanisms with classical Hebbian LTP, as HFS-induced LTP occluded PPT-induced LTP and vice versa. In addition, activity-dependent LTP was blocked by the ERα antagonist, suggesting that ERα activation is involved in NMDA-LTP at TA-CA1 synapses.

Conclusions:

ERα induces a novel form of long-term potentiation at juvenile male hippocampal TA-CA1 synapses. As TA-CA1 synapses are implicated in episodic memory processes, and are an early target for neurodegeneration, these findings have important implications for the role of estrogens in CNS health and neurodegenerative disease.

Keywords: ERα; synaptic plasticity, temporoammonic; AMPA receptor trafficking; estrogen

Introduction.

Numerous studies indicate that estrogens influence hippocampal synaptic function, as 17β estradiol (E2) rapidly potentiates excitatory synaptic transmission at classical Schaffer collateral (SC)-CA1 synapses (Teyler et al, 1980; Wang and Moss, 1992). The effects of E2 are primarily mediated by activation of two estrogen receptors, ERα and ERβ that are differentially expressed in the CNS and have distinct functional roles. Several studies support a role for ERβ in mediating E2 effects at SC-CA1 synapses, as ERβ enhances synaptic plasticity and promotes AMPA receptor (AMPAR) trafficking to synapses (Liu et al, 2008). ERβ also mediates E2-induced rapid changes in dendritic morphology (Srivastava et al, 2010). However, ERα also enhances excitatory synaptic transmission at SC-CA1 synapses (Oberlander and Woolley, 2017).

In addition to the SC input, CA1 pyramidal neurons are innervated by the temporoammonic (TA) pathway that arises in layer III of the entorhinal cortex and forms a direct connection to the stratum lacunosum-moleculare (SLM) region of CA1 neurons. Excitatory synaptic transmission at TA-CA1 synapses is regulated by many neuromodulators, including leptin (Luo et al, 2015) and dopamine (Otmakhova & Lisman 1999). TA-CA1 synapses play a role in hippocampus-dependent memory processes, including spatial novelty detection and memory consolidation (Vago and Kesner, 2008; Remondes and Schuman, 2004). The TA input to CA1 neurons is also implicated in episodic memory as it integrates information from cortical regions and regulates place cell activity (Stokes et al, 2015). This input is also linked to CNS disease as the TA pathway is an early site for tau pathology in Alzheimer's disease (AD; Buxbaum et al, 1998). However, the impact of E2 on excitatory synaptic transmission at TA-CA1 synapses is unclear. Although E2 regulates synaptic transmission at adult TA-CA1 synapses (Smith et al, 2016), the acute actions of E2 at juvenile TA-CA1 synapses are unknown.

Here, E2 induced a persistent increase in excitatory synaptic transmission (LTP) at juvenile male TA-CA1 synapses; an effect mirrored by the ERα agonist, PPT. LTP induced by E2 and PPT was blocked by ERα, not ERβ, antagonists, suggesting a role for ERα. ERα-induced LTP involves a postsynaptic expression mechanism and activation of GluN2B-containing NMDARs as well as PI 3-kinase signalling. Synaptic insertion of GluA2-lacking α-amino-3-hydroxy-5-methyl-4-isoxazolepropionic acid receptors (AMPARs) underlies ERα-induced LTP in slices, and PPT increased trafficking of GluA1 to synapses in hippocampal neurons.

ERα-induced LTP shares similar expression mechanisms to activity-dependent LTP as PPT-induced LTP was occluded by activity-dependent LTP and vice versa. Activity-dependent LTP was blocked by the ERα antagonist, indicating that ERα activation underlies NMDA-LTP at this synapse. These findings suggest an important role for ERα at TA-CA1 synapses, which has important implications for the role of estrogens in health and disease.

Abbreviations.

aCSF: artificial cerebrospinal fluid

AD: Alzheimer's disease

AMPAR: α-amino-3-hydroxy-5-methyl-4-isoxazolepropionic acid receptors

D-AP5: D-2-amino-5-phosphonopentanoate

DPN: Diarylpropionitrile

E2: 17β estradiol

ERα: Estrogen receptor α

ERβ: Estrogen receptor β

HFS: High frequency stimulation

LTP: long-term potentiation

MPP: 1,3-*Bis*(4-hydroxyphenyl)-4-methyl-5-[4-(2-piperidinyl-ethoxy)phenol]-1*H*-pyrazole dihydrochloride

NMDA: N-methyl-D-aspartate

PHTPP: 4-[2-Phenyl-5,7-*bis*(trifluoromethyl)pyrazolo[1,5-*a*]pyrimidin-3-yl]phenol

PhTx: philanthotoxin

PI 3-kinase: phosphoinositide 3-kinase

PPR: paired-pulse facilitation ratio

PPT: 4,4',4''-(4-Propyl-[1H]-pyrazole-1,3,5-triyl)trisphenol

SC: Schaffer collateral

SLM: stratum lacunosum-moleculare

TA: temporoammonic

Bullet Point Summary:

What is already known:

- Estrogens regulate excitatory synaptic transmission at hippocampal CA1 synapses.
- The ER subtypes mediating the regulatory actions of estrogens at TA-CA1 synapses are not clear.

What this study adds:

- ERα activation induces a novel form of LTP at juvenile male TA-CA1 synapses.
- ERα-induced LTP is NMDAR dependent and involves AMPAR trafficking to synapses.

Clinical Significance.

- TA-CA1 synapses are an early target for degeneration in Alzheimer's disease.
- ERα regulation of TA-CA1 synapses has important implications for CNS health and disease.

Materials and Methods

Electrophysiology

All experiments on animals were performed according to UK laws (Scientific Procedures Act 1986) and are reported in compliance with the ARRIVE guidelines (Kilkenny et al., 2010). All experimental procedures on animals were approved by the Animal Welfare Ethical Review Committee at the University of Dundee. Parasaggital hippocampal slices (350 µm) were prepared from P11-P24 old male, Sprague-Dawley (RRID:RGD_5508397) rats as before (Luo et al, 2015). Animals were killed by cervical dislocation in accordance with Schedule 1 of the UK Scientific Procedures Act 1986. Brains were rapidly removed and placed in ice-cold artificial CSF (aCSF; bubbled with 95% O_2 and 5% CO_2) containing the following (in mM): 124 NaCl, 3 KCl, 26 $NaHCO_3$, 1.25 NaH_2PO_4, 2 $CaCl_2$, 1 $MgSO_4$, and 10 D-glucose. Once prepared, slices were allowed to recover at room temperature in oxygenated

aCSF for 1 h before transferring to a submerged chamber maintained at room temperature and perfused with oxygenated aCSF. In all slices, the dentate gyrus and CA3 region were removed to prevent indirect stimulation of the SC input.

Standard extracellular recordings of local field excitatory postsynaptic potentials (fEPSPs) were used to monitor excitatory synaptic transmission at TA-CA1 synapses. Recording pipettes contained aCSF (3-5 MΩ) and were placed in SLM to record TA-CA1 responses. The direct TA pathway was stimulated at 0.033 Hz, using a stimulus intensity that evoked a peak amplitude ~50% of the maximum. Synaptic field potentials were low-pass filtered at 2 kHz and digitally sampled at 10 kHz. The slope of the evoked fEPSPs was expressed relative to the preconditioning baseline. Data were monitored on-line and analyzed off-line using the WinLTP 2.20 program (RRID:SCR_008590; Anderson and Collingridge, 2015). Recording of data was not blinded to the operator, as each electrophysiology experiment required an awareness by the experimenter of the running protocol. In all electrophysiology experiments, fEPSP baseline recordings were only considered stable when both peak amplitude and slope value measurements did not deviate more than 10% from each other. If baseline recordings were not stable, no drug treatment was initiated. The magnitude of LTP induced by ERs was calculated 50-55 min after addition of selective agonists and expressed as a percentage of baseline ± SEM. Activity-dependent LTP was induced by delivery of a high frequency stimulation (HFS; 100Hz/s) paradigm, and as reported previously, blockade of GABAergic inhibition was not required (Luo et al, 2015). All data are expressed as means ± SEM, and statistical analyses were performed using paired *t* test (two-tailed; 95% confidence interval) or repeated-measures ANOVA for comparison of means within subject or one-way ANOVA with Tukey's post hoc test for comparisons between multiple groups. $P < 0.05$ was considered significant. Data analysis was not blinded, but was double checked by more than one researcher. All electrophysiology experiments were performed from $n \geq 5$ slices for each group. Each n value represents an individual slice taken from a separate animal, which is considered to be sufficient for the evaluation of statistical difference in our recordings.

Hippocampal cell culture

Hippocampal cultures were prepared as previously (McGregor et al, 2018). Neonatal Sprague Dawley rats (1-3 days old) were killed by cervical dislocation in accordance with Schedule 1 of UK Animals Scientific Procedures Act (1986). Hippocampi were removed and following washing in HEPES buffered saline (HBS) comprising (in mM): 135 NaCl; 5 KCl; 1 $CaCl_2$; 1 $MgCl_2$; 10 HEPES; 25 D-glucose (pH 7.4), were treated with papain (1.5 $mgml^{-1}$; Sigma

Aldrich, UK) for 20 min at 37°C. Dissociated cells were plated onto sterile dishes (35 mm diameter; Greiner Bio-One Ltd., UK) treated with poly-d-lysine (20 $\mu g ml^{-1}$; 1-2 h) at a density of $5x10^5$ cells/ml. Cultures were maintained in Neurobasal-A medium (Thermofisher Scientific; UK) in a humidified atmosphere of 95% O_2 and 5% CO_2 at 37°C for up to 2 weeks.

Immunocytochemistry

Immunocytochemistry was performed on 7-15 day old cultured hippocampal neurons and all immunocytochemical procedures and analyses comply with the recommendations of Alexander et al (2018). Before labelling, neurons were washed with HBS containing glycine (0.01 mM) and treated with PPT for 15 min at 21-23 °C. For antagonist experiments, neurons were pre-treated with inhibitors for 30 min prior to PPT. To label surface GluA1, living neurons were incubated with an antibody against the N-terminal region of GluA1 (1:100; Moult et al, 2010) at 4°C. Neurons were then fixed with 4% paraformaldehyde for 5 min and surface GluA1 immunostaining was visualised by addition of an anti-sheep Alexa 488-conjugated secondary antibody (1:250; Life Technologies, UK) for 30 min. In a subset of experiments, neurons were permeabilized with 0.1% Triton X-100 (5 min) after fixation. A second primary antibody was then applied to compare GluA1 surface immunostaining relative to PSD-95 (mouse anti-PSD-95; 1:500; Thermo Fisher, UK). An Alexa 568-conjugated anti-mouse secondary antibody (1:200; ThermoFisher, UK) was used to visualize PSD-95 labelling as before (McGregor et al, 2017). No labelling was observed after incubation with secondary antibodies.

Confocal Analysis

A confocal imaging system (Zeiss LSM 510) was used for image acquisition and 488nm and 543nm laser lines was used to excite the Alexa 488 and 555 or 568 fluorophores, respectively. Images were obtained in a single-tracking mode or multi-tracking mode for dual labelling experiments using a 15s scan speed. Intensity of staining was determined offline using Lasersharp software (Carl Zeiss). Analysis lines (50 μm) were drawn along randomly selected dendritic regions and mean fluorescence intensity for GluA1 was calculated for each dendrite (McGregor et al, 2018). For synaptic co-localisation experiments, surface GluA1 immunolabelling was compared with dendritic PSD-95 immunostaining and the number of GluA1-positive sites that co-localised with PSD-95-positive sites were expressed as % of PSD-95-positive sites (McGregor et al, 2018). Data were obtained from at least 3 dendrites

from a minimum of 4 randomly selected neurons for each treatment and from at least 3 different cultures from different animals. Within a given experiment, all conditions were kept constant. Data were normalised relative to mean fluorescence intensity in control neurons. All data are expressed as means ± SEM and statistical analyses were performed using one-way ANOVA for comparisons between multiple groups. $P < 0.05$ was considered significant with *n* representing the number of analysed dendrites.

Data and Statistical Analysis.

The data and statistical analysis comply with the recommendations of the *British Journal of Pharmacology* on experimental design and analysis (Curtis et al, 2018). No power analysis, randomization, or blinding of the samples was performed under recording. The exact group size (*n*) for each experimental group/condition signifies independent values, not replicates. Normality of all data was verified using the Kolmogorov-Smirnov test. To allow for comparison between individual data sets, all data has been normalised. In electrophysiology experiments, data was normalised to the mean slope value of the initial baseline recording and expressed as percentage means ± SEM. In immunocytochemistry experiments, data was normalised to mean intensity value of control neurons and expressed as percentage means ± SEM. In all studies statistical differences were evaluated when $n \geq 5$, and a Tukey's multiple comparison test was used following one-way ANOVA to compare all pairwise whereas a Dunnett's multiple comparison test was used following one-way ANOVA to compare every group with the control group. Post hoc tests were conducted only if *F* was significant and there was no variance inhomogeneity.

Drugs

All drugs were dissolved in aCSF and applied in the bath at the desired final concentration (see table 1). Drugs used were dopamine, 17β-estradiol (E2), 4,4',4"-(4-Propyl-[1H]-pyrazole-1,3,5-triyl)trisphenol (PPT), Diarylpropionitrile (DPN), 1,3-*Bis*(4-hydroxyphenyl)-4-methyl-5-[4-(2-piperidinyl-ethoxy)phenol]-1*H*-pyrazole dihydrochloride (MPP), 4-[2-Phenyl-5,7-*bis*(trifluoromethyl)pyrazolo[1,5-*a*]pyrimidin-3-yl]phenol (PHTPP), D-2-amino-5-phosphonopentanoate (D-AP5), wortmannin, LY294002, PD98059, U0126, PhTx (philanthotoxin), letrozole, NVP-AAM077, ifenprodil, picrotoxin and CGP55845.

Nomenclature of Targets and Ligands

Key protein targets and ligands in this article are hyperlinked to corresponding entries in http://www.guidetopharmacology.org, the common portal for data from the IUPHAR/BPS Guide to PHARMACOLOGY (Harding *et al.*, 2018), and are permanently archived in the Concise Guide to PHARMACOLOGY 2017/18 (Alexander *et al.*, 2017).

Results

E2 rapidly modulates excitatory synaptic transmission at TA-CA1 synapses.

Estrogens modulate excitatory synaptic transmission at SC-CA1 synapses (Oberlander and Woolley 2018; Smejkalova and Woolley; 2010), but the effects of estrogens at TA-CA1 synapses are less clear. To evaluate if estrogens influence TA-CA1 synapses, the effects of E2 were assessed in slices from juvenile male rats. Application of 1μM E2 (15 min) caused an increase in excitatory synaptic transmission (LTP; n=5; F[1,4]=168.973; $p<0.05$; Fig 1A) that was sustained following E2 washout (up to 1hr). As E2 activates different ERs, the role of ERα and ERβ were addressed. To verify the role of ERα, the effects of the ERα antagonist, 1,3-*Bis*(4-hydroxyphenyl)-4-methyl-5-[4-(2-piperidinyl-ethoxy)phenol]-1*H*-pyrazole dihydrochloride (MPP) were assessed. Addition of 1 μM MPP (60 min) had no effect on synaptic transmission (96±1.7% of baseline; n=5; F[1,4]= 0.644, p>0.05), but in MPP-treated slices, the ability of E2 to induce LTP was blocked (n=5; F[1,4]=0.269; p>0.05; Fig 1B). To clarify involvement of ERβ, the effects of the ERβ antagonist, 4-[2-Phenyl-5,7-*bis*(trifluoromethyl) pyrazolo[1,5-*a*]pyrimidin-3-yl]phenol (PHTPP) were examined. Addition of PHTPP (1μM; 60 min) had no effect on synaptic transmission (103±2.3 of baseline; n= 5; F[1,4]= 1.230; p>0.05), and in PHTPP-treated slices, E2 increased synaptic transmission (n=5; F[1,4]= 14.547; p<0.05; data not shown). These data indicate that E2 induces LTP at TA-CA1 synapses via ERα activation. As dopamine selectively depresses excitatory synaptic transmission at TA-CA1synapses (Otmakhova & Lisman 1999), 100μM dopamine was applied at the end of experiments to confirm TA stimulation (Luo et al, 2015).

PPT induces LTP at TA-CA1 synapses via activation of ERα

ERα and ERβ are differentially distributed throughout the hippocampus and divergent effects of ERs at SC-CA1 synapses have been reported (Oberlander and Woolley 2018). As our data suggests that LTP is induced by ERα activation, we examined the role of ERα using the ERα-selective agonist, 4,4',4''-(4-Propyl-[1H]-pyrazole-1,3,5-triyl)trisphenol (PPT). Application

of 25nM PPT increased synaptic transmission (n=5*;* F[1,4]=22.614; *p<0.05*, Fig1C); an effect sustained after washout for up to 60 min. Similarly, 50nM PPT caused a persistent increase in synaptic transmission (140±13.7% of baseline; n=5; F[1,4]=18.866*; p<0.05*). These data indicate that PPT induces a novel form of LTP at TA-CA1 synapses.

To further verify ERα involvement, the effects of the ERα antagonist, MPP were assessed. Application of 1μM MPP (60 min) had no effect on synaptic transmission (n=5; F[1,4]= 0.644; *p>0.05*). However, in the presence of MPP, PPT (25nM) failed to increase synaptic transmission (n=5; *p>0.05;* F[1,4]= 2.814; Fig 1D,F), and this effect was significantly different to PPT-induced LTP (to 131 ± 5.3% of baseline; n=5; F[1,4]=23.397, *p<0.05*).

As ERβ also regulates SC-CA1 synapses (Oberlander and Woolley, 2018; Kramar et al, 2009; Wang et al, 2016), the effects of the ERβ agonist, DPN were compared. Application of 10nM DPN (15 min) had no effect on synaptic transmission (n=6; F[1,5]= 5.591; p>0.05, Fig1E). Addition of other concentrations of DPN also had no effect as synaptic transmission was 101 ± 1.1% of baseline (n=5; F[1,4]= 1.8; p>0.05) and 98 ± 0.7% of baseline (n=5; F[1,4]=1.202; p>0.05) in the presence of 1nM or 25nM DPN, respectively. To explore the role of ERβ further, the effects of the ERβ antagonist, PHTPP were examined. PHTPP (1μM) had no effect on basal synaptic transmission (n=5; F[1,4]= 1.230; p>0.05). Moreover in PHPTT-treated slices, PPT (25nM) evoked a significant increase in synaptic transmission (n=5; F[1,4]=14.840; *p<0.05;* Fig1F). These data indicate that the ability of PPT to induce LTP involves activation of ERα.

PPT-induced LTP has a post-synaptic locus of expression.

As ERα is highly expressed within presynaptic terminals and at postsynaptic densities (McEwen and Milner, 2017; Waters *et al.*, 2009), activation of ERα at either locus may contribute to PPT-induced LTP. To address the locus of PPT-induced LTP, the paired-pulse facilitation ratio (PPR) was analysed as changes in PPR typically reflect alterations in release probability. Paired-pulse facilitation was induced by delivering two pulses at a 50 ms interval. In slices where PPT (25nM) increased synaptic transmission (n=5; F[1,4]= 15.876; *p<0.05*; Fig 2A), no significant change in the PPR was observed (n=5; F[1,4]= 0.823; *p>0.05;* Fig 2B), indicating a likely postsynaptic expression mechanism. As a control, the effects of dopamine were compared as dopamine depresses excitatory synaptic transmission at TA-CA1 synapses via a presynaptic mechanism (Otmakhova and Lisman, 1999). Application of dopamine (100μM) resulted in depression of synaptic transmission which was

accompanied by a significant increase in PPR (n=5; F[1,4]= 38.923; *p<0.05;* Fig 2B). Overall these data indicate that PPT-induced LTP at TA-CA1 synapses involves a postsynaptic expression mechanism.

NMDAR activation is required for PPT-induced LTP.

As synaptic activation of NMDARs is crucial for activity-dependent hippocampal synaptic plasticity (Bliss and Collingridge, 1993), and E2 induces an NMDAR-dependent form of LTP at adult TA-CA1 synapses (Smith *et al.*, 2016), the role of NMDARs were examined using the competitive NMDAR antagonist, D-AP5. Application of 50 μM D-AP5 (60 min) had no effect on basal synaptic transmission (102 ± 0.9% of baseline; n=5; F[1,4]= 1.217*; p>0.05).* However, in the presence of D-AP5, PPT (25nM) failed to alter synaptic transmission (n=5; F[1,4]= 2.578*; p>0.05;* Fig 2C), and this effect was significantly different to the magnitude of PPT-induced LTP (n=5 F[1,4]= 14.482; *p<0.05*). These data suggest that activation of NMDARs is required for PPT-induced LTP.

Different GluN2 subunits determine the biophysical and pharmacological properties of NMDARs, and have differential roles in synaptic plasticity (Paoletti, Bellone and Zhou, 2013). As E2-induced LTP at adult TA-CA1 synapses involves recruitment of GluN2B subunits (Smith *et al.*, 2016), the role of different NMDAR subunits was examined using selective antagonists. Application of ifenprodil (GluN2B antagonist; 3μM) or NVP-AAM077 (putative GluN2A antagonist; 100nM) had no effect on basal synaptic transmission (n=5 for each*;* F[1,4]= 0.386*; p>0.05* and F[1,4]= 0.137; *p>0.05*, respectively*).* In control slices, PPT (25nM) increased synaptic transmission (to 139 ± 8.8% of baseline; n=5; F[1,4]= 16.782; *p<0.05*). In interleaved slices treated with NVP-AAM007, a significant increase in synaptic transmission (*n=5,* F[1,4]= 86.611; *p<0.05;* Fig 2E) was induced by PPT. However, in slices treated with ifenprodil, PPT failed to significantly alter synaptic transmission (n=5; F[1,4]= 0.730; *p>0.05;* Fig 2D), suggesting that GluN2B-containing NMDARs are required for ERα-induced LTP.

As stimulating the TA pathway can activate gamma-aminobutyric acid (GABA)ergic interneurons, which synapse onto CA1 pyramidal cells (Dvorak-Carbone and Schuman, 1999), GABAergic inhibition may play a role in ERα-induced LTP. To explore this, the effects of the $GABA_A$ and $GABA_B$ receptor antagonists, picrotoxin (50 μM) and CGP55845 (100nM) were

examined. In slices, co-application of picrotoxin and CGP55845 had no effect on basal synaptic transmission (100 ± 3.3% of baseline, n =5; F[1,4]= 0.792; p > 0.05). In control slices, application of PPT induced LTP as synaptic transmission increased (to 146 ± 6.0% of baseline; *n=5;* F[1,4]= 68.320; *p<0.05*). However the ability of PPT to induce LTP was unaffected when GABAergic inhibition was blocked, as PPT significantly increased synaptic transmission (to 133 ± 11% of baseline; n = 5; F[1,4]= 14.235; p < 0.05; data not shown) in picrotoxin- and CGP55845-treated slices. These data indicate that ERα-induced LTP at TA-CA1 synapses is independent of $GABA_A$ and $GABA_B$ receptors.

Insertion of GluA2-lacking AMPARs underlies PPT-induced LTP

NMDAR activation promotes AMPAR trafficking and insertion of GluA2-lacking AMPARs into SC-CA1 synapses during LTP (Collingridge et al, 2004). To verify the role of AMPAR trafficking, the effects of PhTx, an inhibitor of GluA2-lacking AMPARs, were assessed. Application of 1μM PhTx (60 min) had no effect on basal synaptic transmission (n=5; F[1,4]= 0.556; *P>0.05).* In control slices, application of PPT increased synaptic transmission (n=5; F[1,4]= 12.270; *p<0.05*; Fig 3A), but, in slices incubated with PhTx (1μM; 90min), PPT failed to alter synaptic transmission (n=5; F[1,4]= 0.699*; p>0.05*; Fig 3B). Application of PhTx immediately after PPT application reversed PPT-induced LTP such that the initial PPT-induced increase in synaptic transmission (n=5; F[1,4]=66.997; *P<0.05)* was returned to baseline levels after Phtx (n=5; F[1,4]= 3.833; *p>0.05;* Fig 3C). Conversely, addition of PhTx, 45 min after PPT, had no effect on PPT-induced LTP (n=5; F[1,4]= 31.008; *p<0.05;* Fig 3D), indicating that insertion of GluA2-lacking AMPARs is key for induction, but not maintenance, of ERα-induced LTP.

Our data suggest that insertion of GluA1-containing AMPARs into TA-CA1 synapses underlies ERα-induced LTP. To directly verify the role of AMPAR trafficking, the effects of PPT on the cell-surface expression of AMPA receptors were assessed using an antibody against the N-terminal domain of GluA1 in cultured hippocampal neurons (McGregor et al, 2017; Moult et al, 2010). Application of 25nM PPT (15 min) resulted in a significant increase in GluA1 surface immunostaining (n=48; F[1,95]= 108.514; *p<0.05).* To verify involvement of ERα, the effects of the ERα antagonist, MPP were evaluated. Treatment with 1μM MPP (15 min) had no effect on GluA1 surface expression (n=48; F[1,95]= 1.345; *p>0.05*; Fig 3E,F). However in MPP-treated neurons, the ability of PPT (25nM) to alter AMPAR trafficking was inhibited, as GluA1 surface expression was not significantly different to control, in neurons

treated with PPT plus MPP (n=48; F[1,95]= 5.078; *p>0.05*; Fig 3E,F). These data indicate that ERα activation increases GluA1 surface expression in hippocampal neurons.

As excitatory synaptic strength depends on AMPAR density at synapses, we determined if ERα activation alters the synaptic expression of GluA1, using dual labelling techniques to compare surface -`GluA1 relative to synapses (anti-PSD-95 antibody) in cultured hippocampal neurons (McGregor et al, 2018). Treatment with PPT (25nM) increased surface GluA1 labelling (to 183 ± 9.6% of control; n = 36; F[1,71]=43.934; *p <0.05*) and increased surface GluA1 that co-localised with PSD-95 (n =36; F[1,71]=191.462; *p <0.05*; Fig 3G). These data indicate that activation of ERα increases the synaptic expression of GluA1 in hippocampal neurons.

As NMDAR activation promotes the synaptic insertion of AMPAR during LTP (Collingridge et al., 2004) and PPT-induced LTP at TA-CA1 synapses is NMDAR dependent, the effects of the NMDAR antagonist, D-AP5, were examined. Treatment with D-AP5 (50 μM) had no effect on surface GluA1 labelling (100 ± 4.3% of control; n=36; F[1,71]=0.114; $p > 0.05$). In control neurons, application of 25nM PPT increased GluA1 surface staining (to 174 ± 7.0% of control; n=36*;* F[1,71]=70.548*; p<0.05),* but in D-AP5-treated neurons, the ability of PPT to enhance GluA1 surface labelling was significantly reduced as PPT failed to enhance GluA1 surface expression in the presence of D-AP5 (to 84 ± 2.9% of control; n=36; F[1,71]=6.730*; p>0.05*). These data indicate that the ERα-driven increase in AMPAR trafficking is NMDAR-dependent.

PPT-induced LTP involves PI 3-kinase signalling

As rapid activation of estrogen receptors stimulates various downstream signalling cascades, including ERK and PI 3-kinase (Titolo *et al.*, 2008; Astous *et al.*, 2006; Smith *et al.*, 2016), the role of these signalling cascades was investigated. To assess the role of PI 3-kinase, two distinct inhibitors of PI 3-kinase were used. Application of either wortmannin (50nM) or LY294002 (10μM) for 60 min had no effect on basal synaptic transmission *(*n=5 for each; F[1,4]= 1.362; *p>0.05* and F[1,4]= 3.845; *p>0.05,* respectively). In interleaved slices, application of PPT (25nM) increased synaptic transmission (n=5; F[1,4]= 25.037; *p<0.*05; Fig 4A**)**. However, in the presence of either PI 3-kinase inhibitor, PPT failed to induce LTP as no significant increase in synaptic transmission was observed after treatment with wortmannin (n=5; F[1,4]= 0.294; *p>0.05;* Fig 4D) or LY294002 (n=5; F[1,4]= 3.231*; p>0.05;* Fig 4B). Conversely, the magnitude of PPT-induced LTP was not altered following

inhibition of ERK with PD98059 or UO126. Application of either ERK inhibitor had no effect on synaptic transmission (n=5 for each; F[1,4]= 2.319; p>0.05 and F[1,4]= 0.143*; p>0.05* respectively), and PPT significantly increased synaptic transmission in slices treated with PD98059 (n=5; F[1,4]= 10.142; p<0.05; Fig 4C) or U0126 (n=5; F[1,4]= 11.890*;* p<0.05; Fig 4D). Together these data indicate that PPT-induced LTP at TA-CA1 synapses involves PI 3-kinase signalling.

To verify that similar signalling pathways underlie ERα regulation of AMPAR trafficking, the role of PI 3-kinase signalling was explored in hippocampal neurons. In control neurons, treatment with PPT (25nM; 15 min) increased GluA1 surface staining (n = 36; F[1,71]=53.331; *p <0.05*; Fig 4E,F). In parallel studies, addition of LY294002 or wortmannin had no effect on surface GluA1 immunostaining (n = 36 for each; F[1,71]=0.305; *p > 0.05* and F[1,71]=1.562; *p>0.05,* respectively; Fig 4E,F). However, in neurons treated with LY294002 or wortmannin, the ability of PPT to increase GluA1 surface expression was inhibited (LY294002: n = 36; F[1,71]=0.091; *p* > 0.05; and wortmannin: *n* = 36; F[1,71]=0.182; *p* > 0.05; Fig 4E,F), indicating that PI 3-kinase signalling is required for PPT-driven alterations in AMPAR trafficking.

PPT-induced LTP occludes HFS-induced LTP at TA-CA1 synapses

LTP is induced at TA-CA1 synapses by high frequency stimulation (HFS) and HFS-induced LTP displays parallels to LTP induced by ERα at TA-CA1 synapses, as both are NMDAR-dependent (Aksoy-Aksel and Manahan-Vaughan, 2015), expressed post-synaptically and require synaptic insertion of GluA2-lacking AMPARs (Luo *et al.*, 2015). Thus, to determine whether PPT-induced LTP and HFS-induced LTP share similar expression mechanisms, occlusion experiments were performed. Initially, a HFS (100Hz; 1s) paradigm was delivered to induce LTP then PPT (25nM) was applied, 30 min after LTP induction. HFS induced LTP (n=5; F[1,4]=33.082; *p<0.05;* Fig 5B); an effect not increased further by subsequent addition of PPT (n=5; F[1,4]= 0.358*; p>0.05*). In parallel studies, PPT (25nM) was initially applied to induce LTP, and this was followed by HFS, 35 min after PPT washout. PPT significantly increased synaptic transmission (n=5; F[1,4]= 223.362; *p<0.05*), but the magnitude of PPT-induced LTP was not altered following HFS (n=5; F[1,4]= 2.147 *p>0.05;* Fig 5A). These data indicate that ERα-induced LTP and activity-dependent LTP at TA-CA1 synapses share similar mechanisms of expression.

ERα activation plays a role in activity-dependent LTP

HFS-induced LTP in young rodents is markedly reduced in the presence of ER antagonist ICI 182 780. Letrozole, which blocks endogenous E2 production by inhibiting P450 aromatase, blocks TBS-induced LTP (Pettorossi *et al* 2013), suggesting that ERs play a role in activity-dependent synaptic plasticity. To assess if ERs are involved in HFS-induced LTP at TA-CA1 synapses, the effects of selective ERα and ERβ antagonists were assessed. Application of either MPP (1μM) or PHTPP (1μM) had no effect on basal synaptic transmission (n=5 for each; F[1,4]= 0.644; *p>0.05* and F[1,4]= 1.230*; p>0.05* respectively). In control slices, delivery of HFS increased synaptic transmission (n=5; F[1,4]= 30.579; *p<0.05;* Fig 5C), but in slices treated with MPP (1μM), HFS failed to induce LTP (n=5; F[1,4]= 0.243*; p>0.05;* Fig 5D) after HFS. Conversely, in slices treated with PHTPP (1μM), robust LTP was observed after HFS (n=5; F[1,4]= 35.912; *p<0.*001; Fig 5E), and this effect was not significantly different (p>0.05) to the magnitude of HFS-induced LTP in interleaved slices (Fig 5F). These data indicate that activation of ERα, but not ERβ, is required for NMDA-dependent LTP at TA-CA1 synapses.

Estrogens can be produced *de novo* in neurons as P450 aromatase, the enzyme involved in E2 synthesis is highly expressed in the brain (Hojo et al 2004). Thus, the involvement of newly synthesised E2 in activity-dependent synaptic plasticity was examined, using the P450 aromatase inhibitor letrozole (Fester et al, 2016). Application of letrozole (100nM; 60min) had no effect on basal synaptic transmission (n=5, F[1,4]= 1.278; *p>0.05).* In control slices, delivery of HFS significantly increased synaptic transmission (n=5; F[1,4]= 22.634*; p<0.05,* Fig 5F). However, in slices treated with letrozole (100nM) for 20 min, subsequent delivery of HFS failed to alter synaptic transmission (n=5, F[1,4]= 0.325; *p>0.05,* Fig 5E,F); an effect significantly different from HFS-induced LTP in control slices (F[1,4]= 15.970; *p<0.05).* Additionally, in slices treated with letrozole (100nM) for 20 min prior to PPT addition, the ability of PPT to induced LTP was not altered, such that application of 25nM PPT evoked a significant increase in synaptic transmission (n=5; F[1,4]= 25.905*; p<0.05*). These data suggest that endogenous production of E2 is required for activity-dependent LTP but does not contribute to PPT-induced LTP at TA-CA1 synapses.

Discussion.

It is known that E2 potentiates excitatory synaptic transmission at SC-CA1 synapses (Smejkalova and Woolley 2010; Smith and McMahon 2005, Smith et al 2009). Previous

studies indicate that E2 is capable of regulating adult female TA-CA1synapses (Smith et al, 2016), however the acute effects of E2 on juvenile male TA-CA1 synapses are unclear. Here we provide the first compelling evidence that E2 activation of ERα induces LTP at TA-CA1 synapses; an effect mirrored by ERα, but not ERβ agonists. ERα-induced LTP is NMDAR-dependent and involves a postsynaptic expression mechanism that requires PI 3-kinase signalling and synaptic insertion of GluA2-lacking AMPA receptors (Fig 6). ERα-induced LTP has overlapping expression mechanisms with classical Hebbian LTP, as HFS-induced LTP occluded PPT-induced LTP and vice versa. Activation of ERα was also involved in NMDA-dependent LTP as antagonism of ERα inhibited HFS-induced LTP at TA-CA1 synapses. Endogenous production of E2 is also required for NMDA-dependent LTP as blockade of E2 synthesis with the aromatase inhibitor, letrozole, blocked HFS-induced LTP at TA-CA1 synapses.

Here we show that the ERα agonist, PPT induces a persistent increase in synaptic efficacy at juvenile male TA-CA1 synapses. Conversely, the ERβ agonist, DPN was without effect. The effects of PPT on synaptic efficacy involve ERα as PPT-induced LTP was blocked by an ERα antagonist indicating that ERα activation mediates LTP induced by PPT. E2 also induced LTP at TA-CA1 synapses, and this effect was blocked by MPP. These findings contrast with previous studies as ERβ enhances excitatory synaptic efficacy at SC-CA1 synapses (Kramar et al, 2009; Oberlander and Woolley 2016), suggesting that the two inputs to CA1 neurons are differentially regulated by ERs. Recent evidence has identified sex differences in the ER subtype mediating E2-induced synaptic potentiation (Oberlander and Woolley 2016). Thus, in addition to distinct ERs regulating synaptic efficacy at the two CA1 synapses, different ERs have distinct regulatory roles in male and female. As our studies were performed in male, an ERα-independent process may regulate TA-CA1 synaptic efficacy in female, although this remains to be determined.

Our data indicate that a postsynaptic expression mechanism underlies PPT-induced LTP as no alteration in PPR was observed after PPT treatment. This contrasts with the ERα-driven increases in excitatory synaptic transmission at male SC-CA1 synapses as this involves a presynaptic mechanism (Oberlander and Woolley, 2016). However, a postsynaptic mechanism underlies the ERβ increase in synaptic transmission at male SC-CA1 synapses (Oberlander and Woolley, 2016). Thus clear differences also exist in the locus and mechanisms of action of different ERs between SC-CA1 and TA-CA1 synapses.

NMDAR activation is critical for LTP induction at SC-CA1 (Bliss and Collingridge, 1993) and TA-CA1 (Luo et al, 2015) synapses. NMDAR activation was also required for PPT-induced LTP as D-AP5 blocked the effects of PPT on synaptic efficacy. NMDARs comprised of different subunits are implicated in different forms of hippocampal synaptic plasticity (Li et al, 2004; Bartlett et al, 2004), and GluN2B subunits are required for HFS-induced LTP at TA-CA1 synapses (McGregor et al 2018). Similarly, PPT-induced LTP is prevented following inhibition of GluN2B subunits, not GluN2A subunits, indicating that activation of GluN2B-containing NMDA receptors is required for PPT-induced LTP. In accordance with these findings, GluN2B subunits are also implicated in E2-mediated regulation of synaptic function at adult female TA-CA1 synapses (Smith et al, 2016).

Synaptic activation of NMDARs is crucial for LTP induction, and synaptic insertion of AMPA receptors during LTP (Collingridge et al, 2004). In support of a role for AMPA receptor trafficking, PPT-induced LTP was blocked by inhibiting GluA2-lacking AMPA receptors with Phtx. However, Phtx failed to reverse established PPT-induced LTP, suggesting that PPT insertion of GluA2-lacking AMPA receptors underlies induction but not maintenance of LTP. Previous studies have identified that ERβ regulates GluA1 trafficking (Liu et al, 2008; Srivastava et al, 2010), as ERβ increases hippocampal GluA1 phosphorylation and surface expression (Liu et al, 2008). Reductions in GluA1 surface expression have also been detected following ERβ activation (Srivastava et al, 2010). Conversely, we show that PPT increased synaptic density of GluA1, and in agreement with others (Man et al, 2003), PI 3-kinase signalling is involved. E2-driven trafficking of AMPARs involves actin polymerisation (Kramar et al, 2009). As PI 3-kinase phosphorylates PIP_2 into PIP_3, and elevated PIP_3 levels stimulates actin polymerisation (Dotti et al 2014), ERα activation may regulate GluA1 trafficking via PI 3-kinase-driven changes in actin dynamics.

Although ERα activation stimulates ERK signalling in hippocampal neurons (Pereira et al, 2014), we found no evidence to support a role for ERK, as inhibition of ERK failed to inhibit PPT-induced LTP. The role of an ERK-independent pathway in ERα-induced LTP contrasts with ERK involvement in E2 regulation of SC-CA1 synapses (Jain et al, 2018; Kumar et al, 2015; Zadran et al, 2009) and adult female TA-CA1 synapses (Smith et al, 2016).

The novel form of LTP induced by ERα displays parallels to activity-dependent hippocampal LTP as synaptic activation of NMDARs and synaptic insertion of GluA2-lacking AMPA

receptors are required for both. Moreover, ERα-induced LTP occluded synaptically-induced LTP and vice versa, indicating that similar expression mechanisms are involved. Treatment with the ERα antagonist, MPP, also prevented HFS-induced LTP suggesting that ERα activation is crucial for LTP induction at TA-CA1 synapses. Moreover, inhibition of aromatase activity also blocked HFS-induced LTP, indicating that endogenous production of E2 is required for activity-dependent LTP at TA-CA1 synapses. These findings are consistent with previous studies demonstrating that rodents treated with letrozole display impairments in hippocampal LTP (Kretz et al 2004; Grassi et al 2011).

Physiological significance.

Numerous studies support a potential cognitive enhancing role for estrogens, as variations in estrogen levels are associated with altered memory function, whereas spatial memory deficits observed in ovariectomised animals are reversed by estrogen (Holmes et al, 2002; Frick and Kim, 2018; Foster et al, 2003). Treatment with E2 also improves retention in hippocampal memory tasks (Gibbs et al, 2008). Several studies have identified a role for ERβ in memory, as ERβ knock-out mice exhibit spatial memory impairments (Liu et al, 2008), whereas ERβ agonists enhance memory performance (Rissman et al, 2002; Rhodes et al, 2006). ERα activation is also linked to memory as Erα knock-out mice display impairments in hippocampus-dependent memory (Fugger et al 1998), whereas lentiviral expression of ERα rescues memory impairments in Erα knock-out mice (Foster et al 2008) and intra-hippocampal infusions of PPT enhance memory (Boulware et al, 2013; Phan et al, 2011). Increased hippocampal expression of ERα in aged animals is also reported to have beneficial effects on hippocampus-dependent memory (Bean et al, 2015). As TA-CA1 synapses are implicated in spatial novelty and formation of episodic memories (Remondes and Schumann, 2004; Stokes et al, 2015), the ability of PPT to induce TA-CA1 LTP may be important for memory consolidation and episodic memory.

The TA pathway degenerates in early AD (Buxbaum et al, 1998), and deficits in synaptic plasticity at TA-CA1 synapses occur in rodent models of AD (Booth et al, 2016). The incidence of AD is higher in women and the hypo-estrogenic state of postmenopausal women is related to AD risk (Barnes et al 2005). Estrogens also influence AD pathology, with alterations in ApoE gene expression detected after estrogen (Strivastava et al 1996) and decreased ERα levels in AD patients (Hu et al 2003). Consequently, as estrogens are linked to

AD pathology, the ability of ERα to regulate TA-CA1 synaptic efficacy has important implications for their role in neurodegenerative disorders.

Author contributions

L.C. performed all the studies and analysed all the data. J.H. designed and supervised the study and drafted the manuscript. All authors took part in correcting the proofs and approved the final manuscript.

Conflicts of Interest.

The authors declare no conflicts of interest.

Declaration of transparency and scientific rigour

This Declaration acknowledges that this paper adheres to the principles for transparent reporting and scientific rigour of preclinical research as stated in the *BJP* guidelines for Design & Analysis, Immunoblotting and Immunochemistry, and Animal Experimentation, and as recommended by funding agencies, publishers and other organisations engaged with supporting research.

References.

Aksoy-Aksel, A. and Manahan-Vaughan, D. (2015) Synaptic strength at the temporoammonic input to the hippocampal CA1 region in vivo is regulated by NMDA receptors, metabotropic glutamate receptors and voltage-gated calcium channels. Neuroscience. 309, 191–199.

Alexander SPH, et al. (2018). Goals and practicalities of immunoblotting and immunohistochemistry: A guide for submission to the British Journal of Pharmacology. Br J Pharmacol. 175, 407-411.

Alexander SPH, et al (2017). THE CONCISE GUIDE TO PHARMACOLOGY 2017/18: Nuclear hormone receptors. British Journal of Pharmacology, 174, S208-224

Anderson WW, Collingridge GL. (2007). Capabilities of the WinLTP data acquisition program extending beyond basic LTP experimental functions. J Neurosci Methods. 162, 346-356.

Barnes LL, Wilson RS, Bienias JL, Schneider JA, Evans DA, Bennet DA. (2005) Sex differences in the clinical manifestations of Alzheimer disease pathology. Archives of General Psychiatry 62, 685-691

Bartlett TE, et al. (2007). Differential roles of NR2A and NR2B-containing NMDA receptors in LTP and LTD in the CA1 region of two-week old rat hippocampus. Neuropharmacology. 52, 60-70.

Bean LA, Kumar A, Rani A, Guidi M, Rosario AM, Cruz PE, Golde TE, Foster TC. (2015). Re-Opening the Critical Window for Estrogen Therapy. J Neurosci. 35, 16077-93.

Bliss, T. V, Collingridge, G. L. (1993). A synaptic model of memory: long-term potentiation in the hippocampus. Nature, 361, 31-39.

Booth C, et al. (2016) Alterations to intrinsic pyramidal neuron properties and temporoammonic synaptic plasticity underlie deficits in hippocampal network function in a mouse model of tauopathy. J Neurosci 36, 350-363

Boulware MI, Heisler JD, Frick KM. (2013). The memory-enhancing effects of hippocampal estrogen receptor activation involve metabotropic glutamate receptor signaling. J Neurosci. 33, 15184-94.

Buxbaum, J.D. et al. (1998). Alzheimer amyloid protein precursor in the rat hippocampus: transport and processing through the perforant path. J. Neurosci. 18, 9629-9637.

Collingridge GL, Isaac JT, Wang YT. (2004). Receptor trafficking and synaptic plasticity. Nat Rev Neurosci. 5, 952-62.

Curtis MJ, Alexander S, Cirino G, Docherty JR, George CH, Giembycz MA, Hoyer D, Insel PA, Izzo AA, Ji Y, MacEwan DA, Sobey CG, Stanford SC, Teixeira MM, Wonnacott S, Ahluwalia A. (2018) Experimental design and analysis and their reporting II: updated and simplified guidance for authors and peer reviewers. Br J Pharmacology 175 987–993.

D'Astous M, Mendez P, Morissette M, Garcia-Segura LM, Di Paolo T. (2006). Implication of the phosphatidylinositol-3 kinase/protein kinase B signaling pathway in the neuroprotective effect of estradiol in the striatum of 1-methyl-4-phenyl-1,2,3,6-tetrahydropyridine mice. Mol Pharmacol. 69(4), 1492-8.

Dotti CG, Esteban JA, Ledesma MD. (2014). Lipid dynamics at dendritic spines. Frontiers in neuroanatomy, 8, 76.

Fester L, Brandt N, Windhorst S, Prols F, Blaute C, Rune GM. (2016) Control of aromatase in hippocampal neurons. J Steroid Biochem Mol Bio. 160, 9-14.

Foster TC, Rani A, Kumar A, Cui L, Semple-Rowland SL. (2008). Viral Vector-mediated Delivery of Estrogen Receptor-α to the Hippocampus Improves Spatial Learning in Estrogen Receptor-α Knockout Mice. Mol Ther. 16, 1587-1593.

Foster TC, Sharrow KM, Kumar A, Masse J. (2003). Interaction of age and chronic estradiol replacement on memory and markers of brain aging. Neurobiol Aging. 24, 839-52.

Frick KM, Kim J. (2018). Mechanisms underlying the rapid effects of estradiol and progesterone on hippocampal memory consolidation in female rodents. Horm Behav. 104:100-110.

Fugger HN, Cunningham SG, Rissman EF, Foster TC. (1998). Sex differences in the activational effect of ERalpha on spatial learning. Horm Behav. 34, 163-70.

Gibbs RB, Johnson DA. (2008). Sex-specific effects of gonadectomy and hormone treatment on acquisition of a 12-arm radial maze task by Sprague Dawley rats. Endocrinology. 149, 3176-83.

Grassi S, et al. (2011). Neural 17β-estradiol facilitates long-term potentiation in the hippocampal CA1 region. Neuroscience. 192, 67-73.

Harding SD, Sharman JL, Faccenda E, Southan C, Pawson AJ, Ireland S *et al.* (2018). The IUPHAR/BPS Guide to PHARMACOLOGY in 2018: updates and expansion to encompass the new guide to IMMUNOPHARMACOLOGY. Nucl Acids Res 46: D1091-D1106.

Hojo Y, et al. (2003). Adult male rat hippocampus synthesizes estradiol from pregnenolone by cytochromes P45017alpha and P450 aromatase localized in neurons. Proceedings of the National Academy of Sciences of the United States of America, 101(3), 865–870.

Holmes MM, Wide JK, Galea LA. (2002). Low levels of estradiol facilitate, whereas high levels of estradiol impair, working memory performance on the radial arm maze. Behav Neurosci. 116, 928-34.

Hu XY, Qin S, Lu YP, Ravid R, Swaab DF, Zhou JN. (2003) Decreased estrogen receptor-α expression in hippocampal neurons in relation to hyperphosphorylated tau in Alzheimer patients. Acta neuropathologica 106, 213-220.

Jain A, Zhe Huang G, Woolley CS. (2019). Latent sex differences in molecular signaling that underlies excitatory synaptic potentiation in the hippocampus. J Neurosci. 39, 1552-1565.

Kilkenny, C, Browne, W, Cuthill, IC, Emerson, M, Altman, DG (2010). Animal research: reporting in vivo experiments: the ARRIVE guidelines. Br J Pharmacol 160, 1577-1579.

Kramár EA, et al. (2009). Cytoskeletal changes underlie estrogen's acute effects on synaptic transmission and plasticity. J Neurosci. 29, 12982-93

Kretz O, et al. (2004) Hippocampal synapses depend on hippocampal estrogen synthesis. JNeurosci, 24, 5913-21.

Kumar A, Bean LA, Rani A, Jackson T, Foster TC. (2015). Contribution of estrogen receptor subtypes, ERα, ERβ, and GPER1 in rapid estradiol-mediated enhancement of hippocampal synaptic transmission in mice. Hippocampus. 25, 1556-66.

Liu F, et al. (2008). Activation of estrogen receptor-beta regulates hippocampal synaptic plasticity and improves memory. Nat Neurosci. 11, 334-43.

Liu L, et al. (2004). Role of NMDA receptor subtypes in governing the direction of hippocampal synaptic plasticity. Science. 304, 1021-4.

Luo, X. McGregor G, Irving A J, Harvey J. (2015). Leptin Induces a Novel Form of NMDA Receptor-Dependent LTP at Hippocampal Temporoammonic- CA1 Synapses. eNeuro, 2, 1-17.

Man HY, et al. (2003). Activation of PI3-kinase is required for AMPA receptor insertion during LTP of mEPSCs in cultured hippocampal neurons. Neuron. 38, 611-24.

McEwen BS, Milner TA. (2017). Understanding the broad influence of sex hormones and sex differences in the brain. J Neurosci Res. 95, 24-39.

McGregor G, Irving AJ, Harvey J. (2017). Canonical JAK-STAT signaling is pivotal for long-term depression at adult hippocampal temporoammonic-CA1 synapses. FASEB J. 31, 3449-3466.

McGregor G, Clements L, Farah A, Irving AJ, Harvey J. (2018). Age-dependent regulation of excitatory synaptic transmission at hippocampal temporoammonic-CA1 synapses by leptin. Neurobiol Aging. 69, 76-93.

Moult PR, et al. (2010). Leptin regulates AMPA receptor trafficking via PTEN inhibition. J Neurosci. 30, 4088-101.

Oberlander JG, Woolley CS. (2016). 17β-Estradiol Acutely Potentiates Glutamatergic Synaptic Transmission in the Hippocampus through Distinct Mechanisms in Males and Females. J Neurosci. 36, 2677-90.

Otmakhova, N. A. and Lisman, J. E. (1999). Dopamine Selectively Inhibits the Direct Cortical Pathway to the CA1 Hippocampal Region. J. Neurosci., 19, 1437-1445.

Paoletti P, Bellone C, Zhou Q. (2013). NMDA receptor subunit diversity: impact on receptor properties, synaptic plasticity and disease. Nat Rev Neurosci. 14, 383-400.

Pereira LM, Bastos CP, de Souza JM, Ribeiro FM, Pereira GS. (2014). Estradiol enhances object recognition memory in Swiss female mice by activating hippocampal estrogen receptor α. Neurobiol Learn Mem. 114, 1-9.

Pettorossi VE, et al. (2013). Modulatory role of androgenic and estrogenic neurosteroids in determining the direction of synaptic plasticity in the CA1 hippocampal region of male rats. Physiol Rep. 1, e00185.

Phan A, Lancaster KE, Armstrong JN, MacLusky NJ, Choleris E. (2011). Rapid effects of estrogen receptor α and β selective agonists on learning and dendritic spines in female mice. Endocrinology. 152, 1492-502.

Qu N., Wang L., Liu Z.-C., Tian Q. & Zhang Q (2013) Oestrogen receptor α agonist

improved long-term ovariectomy-induced spatial cognition deficit in young rats. International Journal of Neuropsychopharmacol. 16, 1071-1082

Remondes M, Schuman EM (2002) Direct cortical input modulates plasticity and spiking in CA1 pyramidal neurons. Nature 416, 736-740

Remondes M, Schuman EM (2004) Role for a cortical input to hippocampal area CA1 in the consolidation of a long-term memory. Nature 43, 699-703

Rhodes ME, Frye CA. (2006). ERbeta-selective SERMs produce mnemonic-enhancing effects in the inhibitory avoidance and water maze tasks. Neurobiol Learn Mem. 85, 183-91.

Rissman EF, Heck AL, Leonard JE, Shupnik MA, Gustafsson JA. (2002). Disruption of estrogen receptor beta gene impairs spatial learning in female mice. Proc Natl Acad Sci U S A. 99, 3996-4001.

Smejkalova T, Woolley CS. (2010). Estradiol acutely potentiates hippocampal excitatory synaptic transmission through a presynaptic mechanism. J Neurosci. 30, 16137-48.

Smith CC, McMahon LL (2005) Estrogen-Induced Increase in the Magnitude of Long-Term Potentiation Occurs Only When the Ratio of NMDA Transmission to AMPA Transmission Is Increased. J.Neurosci 25, 7780-7791.

Smith C C, Vedder LC, McMahon LL. (2009). Estradiol and the relationship between dendritic spines, NR2B containing NMDA receptors, and the magnitude of long-term potentiation at hippocampal CA3-CA1 synapses. Psychoneuroendocrinol. 34, S130-42.

Smith CC, Smith LA, Bredemann TM, McMahon LL. (2016) 17β estradiol recruits GluN2B-containing NMDARs and ERK during induction of long-term potentiation at temporoammonic-CA1 synapses. Hippocampus, 26, 110–117.

Stokes J, Kyle C, Ekstrom AD (2015) Complementary roles of human hippocampal subfields in differentiation and integration of spatial context. J Cogn Neurosci 27, 546–559

Srivastava DP, Woolfrey KM, Liu F, Brandon NJ, Penzes P. (2010). Estrogen receptor ß activity modulates synaptic signaling and structure. J Neurosci. 30, 13454-60.

Srivastava RA, Bhasin N, Srivastava N (1996) Apolipoprotein E gene expression in various of mouse and regulation by estrogen. Biochem Mol Biol Int 38, 91–101.

Teyler TJ, Vardaris RM, Lewis D, Rawitch AB. (1980). Gonadal steroids: effects on excitability of hippocampal pyramidal cells. Science. 209, 1017-8.

Titolo, D. Mayer CM, Dhillon SS, Cai F, Belsham DD. (2008) Estrogen facilitates both phosphatidylinositol 3-kinase/Akt and ERK1/2 mitogen-activated protein kinase membrane signaling required for long-term neuropeptide Y transcriptional regulation in clonal, immortalized neurons. J Neurosci, 28, 6473-6482.

Vago DR, Kesner RP (2008) Disruption of the direct perforant path input to the CA1 subregion of the dorsal hippocampus interferes with spatial working memory and novelty detection. Behav Brain Res 189, 273-283

Waters, E. M. Mitterling K, Spencer JL, Mazid S, McEwen BS, Milner TA. (2009). Estrogen receptor alpha and beta specific agonists regulate expression of synaptic proteins in rat hippocampus, Brain Res. 1290, 1–11.

Wang W, Kantorovich S, Babayan AH, Hou B, Gall CM, Lynch G. (2016). Estrogen's Effects on Excitatory Synaptic Transmission Entail Integrin and TrkB Transactivation and Depend Upon β1-integrin function. Neuropsychopharmacol. 41, 2723-32.

Zadran S, et al. (2009). 17-Beta-estradiol increases neuronal excitability through MAP kinase-induced calpain activation. Proc Natl Acad Sci U S A. 106, 21936-41.

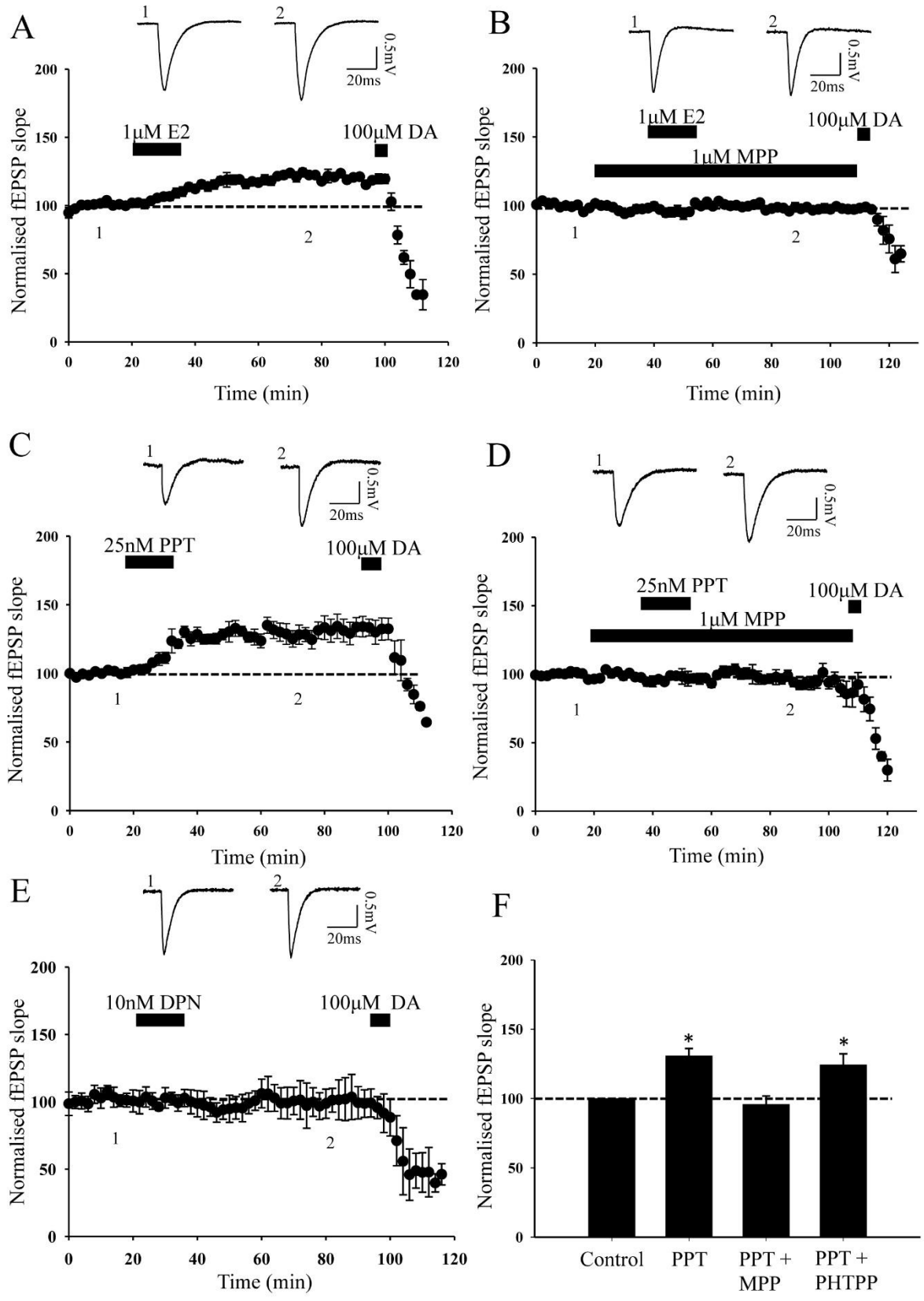

Figure 1. ERα activation induces LTP at juvenile TA-CA1 synapses.

(A-E) Pooled data showing the effects of E2 (1 μM; 15 min, A-B), PPT (25-50 nM; C-D) and DPN (10nM; E) on excitatory synaptic transmission at TA-CA1 synapses in juvenile hippocampal slices. At the end of experiments, application of dopamine (100 μM; 5 min) inhibits synaptic transmission confirming TA stimulation. In this and subsequent figures, each point is the average of 4 successive responses, and representative fEPSPs are shown above each plot and for the time indicated. Application of E2 caused a persistent increase in synaptic transmission (A) that was blocked by selective inhibition of ERα with MPP (B). C, Addition of the ERα agonist, PPT induced a persistent increase in synaptic efficacy; an effect that was blocked by the ERα antagonist, MPP (D). E, In contrast, the ERβ agonist, DPN has no effect on excitatory synaptic transmission. F, Bar chart of pooled data illustrating the effects of PPT alone and in the presence of MPP, or the ERβ antagonist PHTPP, on synaptic transmission. ERα activation induced a novel form of LTP at TA-CA1 synapses.

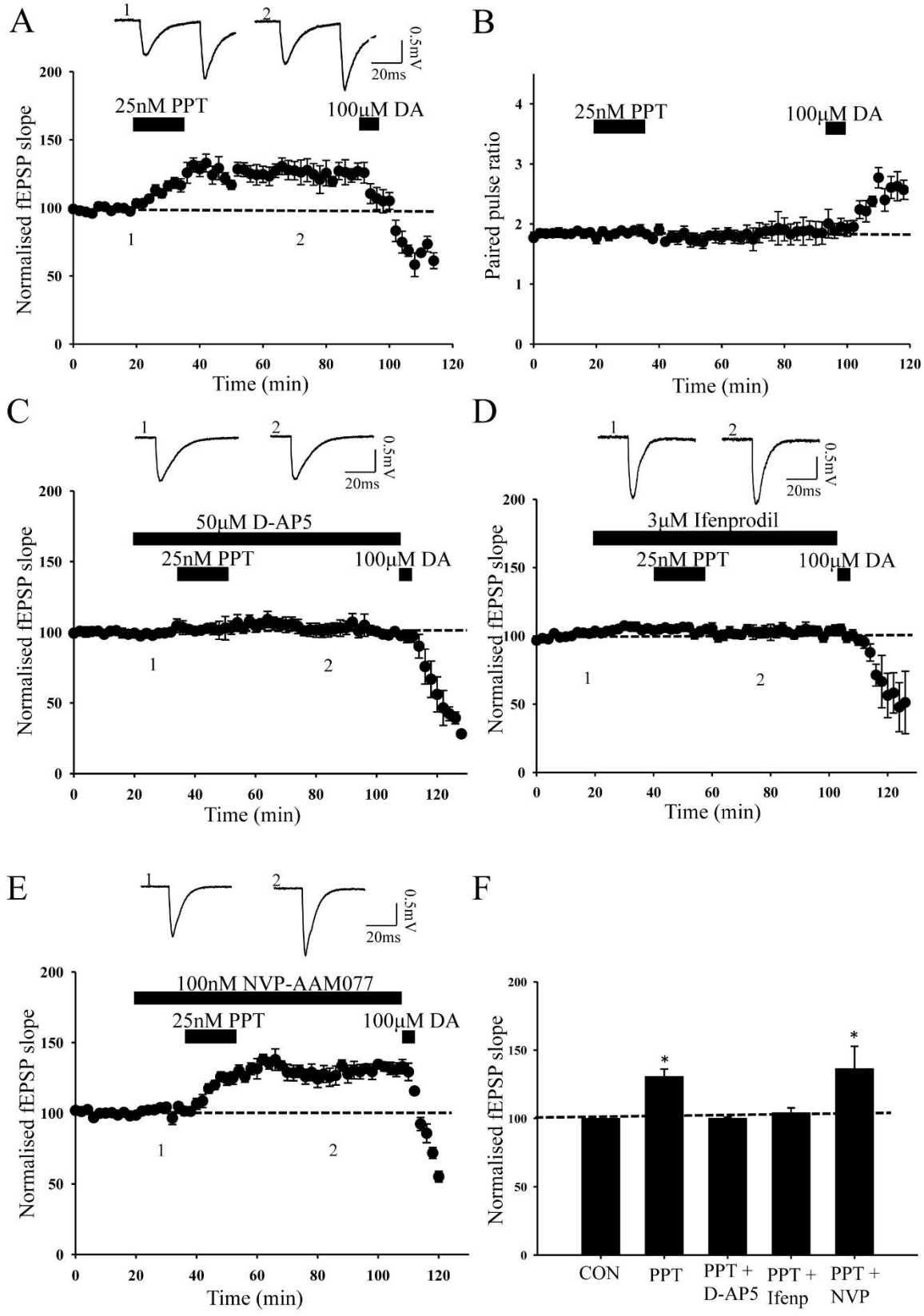

Figure 2. PPT-induced LTP is NMDAR-dependent and involves a postsynaptic expression mechanism.

A, Plot of pooled data illustrating the effects of 25 nM PPT (15 min) on synaptic transmission at TA-CA1 synapses. B, Corresponding plot of the pooled paired pulse ratio (PPR) against time for experiments shown in A. The effects of PPT were not accompanied by any change in PPR, indicating a postsynaptic mechanism. C-E, Plots of pooled data illustrating the effects of PPT (25 nM; 15 min) on synaptic transmission in hippocampal slices. NMDAR activation was involved as PPT failed to induce LTP in the presence of the competitive NMDAR antagonist, D-AP5 (50 μM; C). D-E, The ability of PPT to induce LTP was blocked following inhibition of GluN2B subunits with ifenprodil (D), but was unaffected by the GluN2A inhibitor, NVP-AAM0077 (E).

F, Bar chart of pooled data illustrating the relative effects of PPT on synaptic transmission in control conditions and after treatment with D-AP5, ifenprodil or, NVP-AAM0077. PPT-induced LTP involves activation of GluN2B subunits.

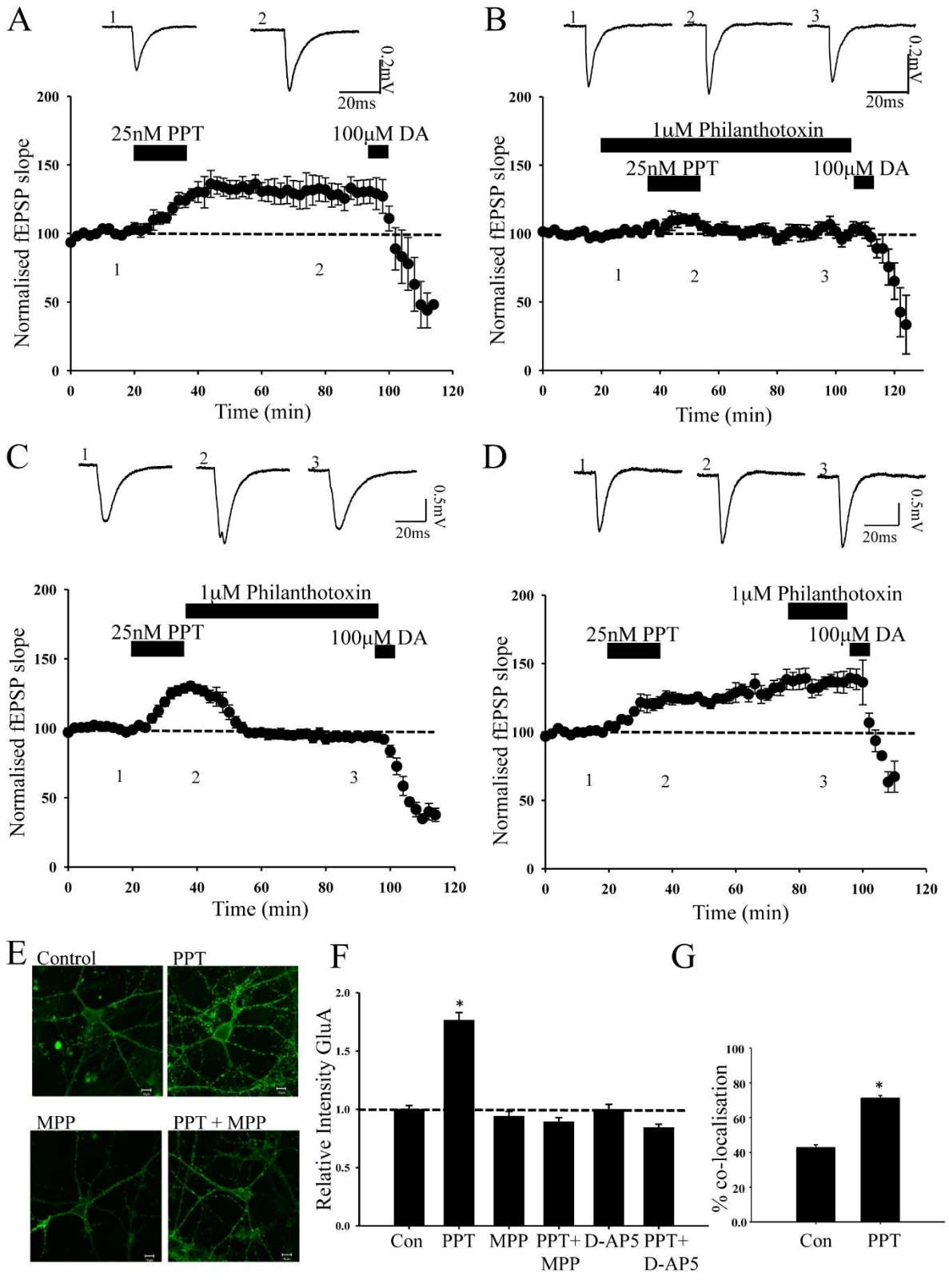

Figure 3. Synaptic insertion of GluA2-lacking AMPARs underlies ERα-induced LTP.

A-D, Plots of pooled data illustrating effects on synaptic transmission in hippocampal slices. A, LTP was evoked by addition of 25 nM PPT, but prior exposure to Phtx (1µM; B), prevented PPT-induced LTP. C, Application of Phtx immediately after addition of PPT, resulted in reversal of PPT-induced. D, Addition of Phtx, 45 min after PPT failed to reverse PPT-induced LTP. E,

Representative confocal images of surface GluA1 labelling in control hippocampal neurons and after PPT, MPP, or PPT plus MPP (DIV7-13). F, Pooled data illustrating the relative effects on GluA1 surface labelling in control conditions, and after addition of PPT, MPP, or PPT plus MPP. ERα activation increases GluA1 surface expression (DIV7-13). G, Pooled data showing the effects on % GluA1/PSD-95 co-localisation. The ERα agonist, PPT increased GluA1 expression at hippocampal synapses (DIV7-13).

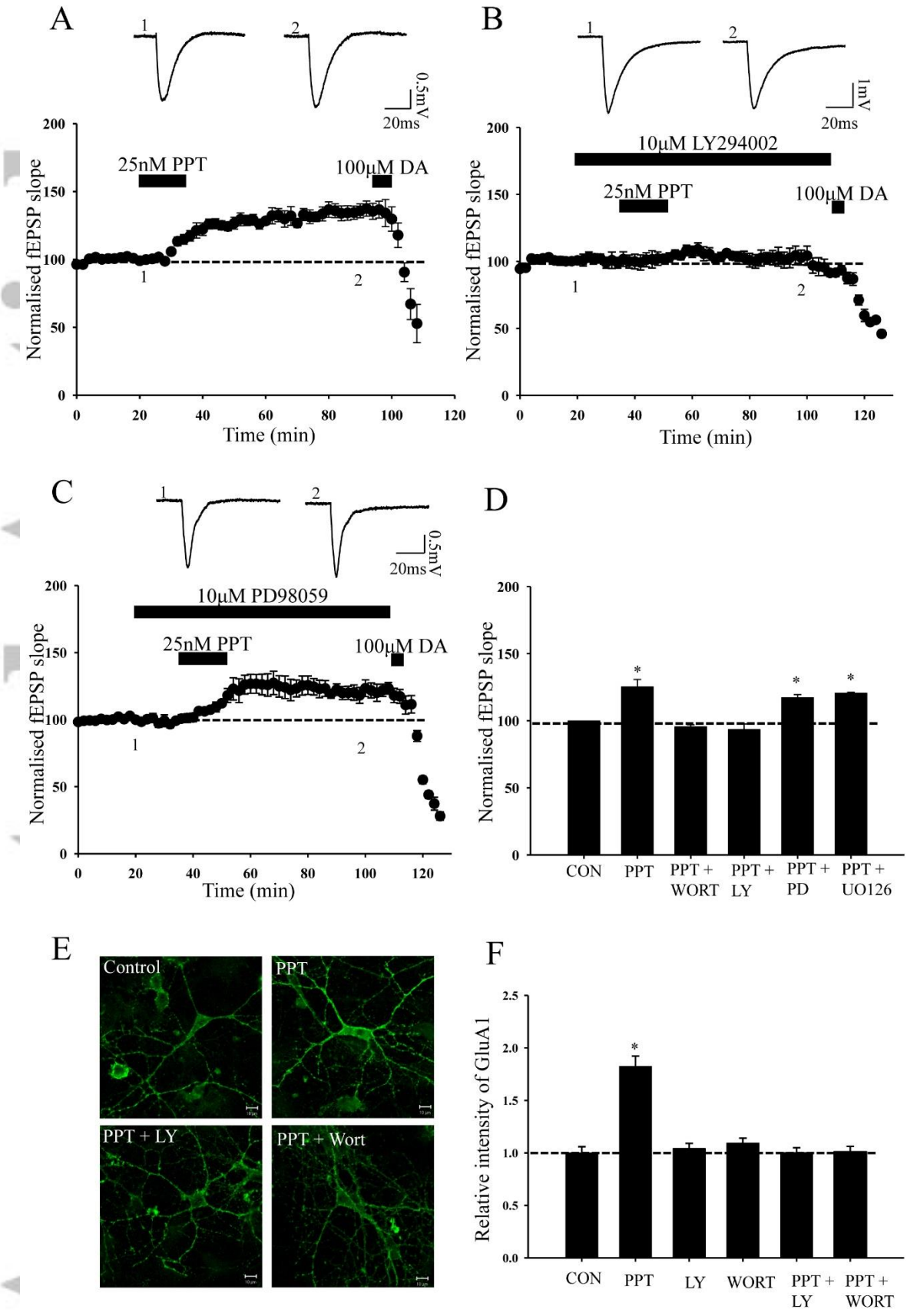

Figure 4. ERα-induced LTP involves PI 3-kinase signalling.

A-C, Pooled data illustrating the effects on excitatory synaptic transmission in slices. The ability of PPT to induce LTP (A) was blocked after PI3K inhibition with LY294002 (B), but was unaffected in the presence of the ERK inhibitor, PD98059 (C). D, Pooled data illustrating the effects of PPT on synaptic transmission in control conditions and after incubation with inhibitors of PI3-kinase (LY294002; wortmannin) or ERK (PD98059; U0126). PPT-induced LTP involves a PI 3-kinase-driven process. E, Representative confocal images of surface GluA1 labelling in control neurons and after PPT, PPT plus LY294002, or PPT plus wortmannin. (DIV8-15) F, Pooled data illustrating the relative effects on GluA1 surface labelling in control conditions, after addition of PPT, and in the combined presence of PPT plus LY294002, or PPT plus wortmannin (DIV8-15). The ability of ERα to increase GluA1 surface expression involves PI 3-kinase signalling.

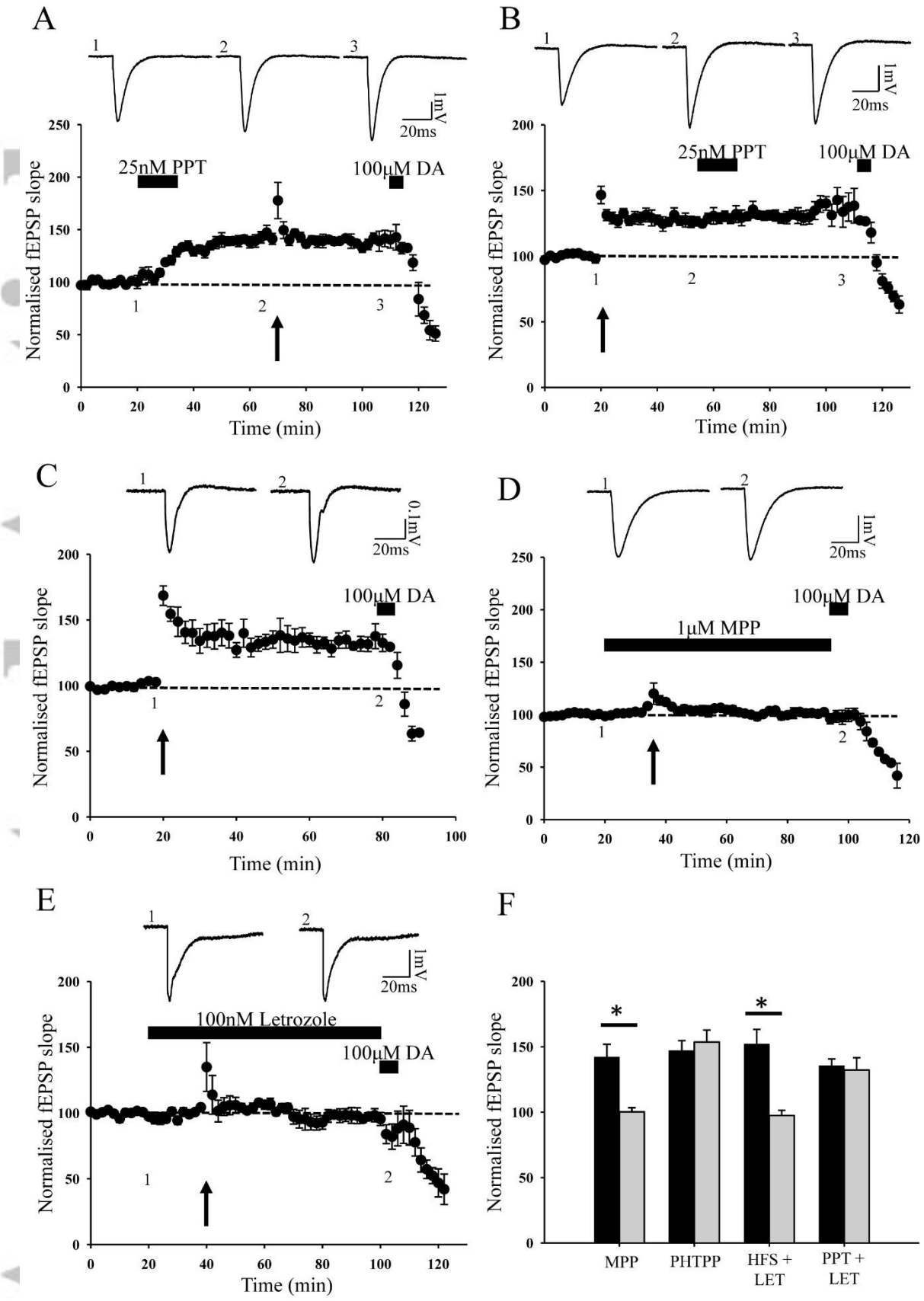

Figure 5. ERα activation is involved in activity-dependent LTP at TA-CA1 synapses.

A-E, Plots of pooled data illustrating effects on synaptic transmission at TA-CA1 synapses. A, Application of PPT induces LTP, however subsequent delivery of HFS (shown by arrow) failed to increase synaptic strength further. B, LTP was evoked by HFS, however subsequent addition of PPT failed to alter synaptic transmission. ERα-induced LTP and activity-dependent LTP at TA-CA1 synapses share similar expression mechanisms. C, In control slices, delivery of HFS induced LTP. D, In interleaved slices treated with MPP, delivery of HFS failed to induce LTP. E, HFS fails to induce LTP in slices treated with letrozole F, Bar chart of pooled data illustrating the effects of HFS on synaptic transmission in control conditions (black bar) and following treatment with either MPP, PHTPP or letrozole (grey bars).

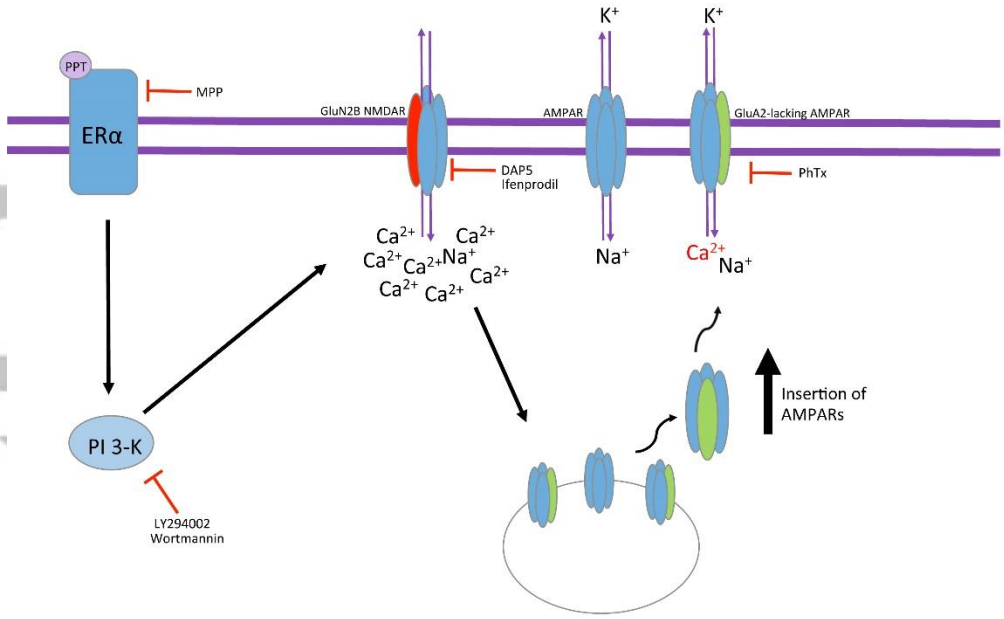

Figure 6. Activation of ERα induces a novel form of NMDA-dependent LTP at juvenile TA-CA1 synapses.

Schematic representation of the key cellular mechanisms involved in the novel form of LTP induced by ERα at juvenile TA-CA1 synapses. Activation of ERα by selective agonists or endogenous E2 results in stimulation of PI 3-kinase signalling. This in turn increases the synaptic activation of GluN2B-containing NMDA receptors which ultimately promote insertion of GluA2-lacking AMPA receptors into hippocampal TA-CA1 synapses.

Table 1. Summary of drugs used.

Drug	Concentration	Biological Activity
17β-estradiol	1μM	Non-selective, estrogen receptor agonist
CGP55845	100nM	$GABA_BR$ antagonist
D-AP5	50μM	Competitive NMDAR antagonist
DPN	1nM, 10nM, 25nM	ERβ agonist
Dopamine	100μM	Neurotransmitter/hormone
Ifenprodil	3μM	GluN2B-NMDAR antagonist
Letrozole	100nM	Aromatase inhibitor
LY294002	10μM	PI3-Kinase inhibitor
MPP	1μM	ERα antagonist
NVP-AAM077	100nM	GluN2A-NMDAR antagonist
PD98059	10μM	ERK inhibitor
Philanthotoxin	1μM	GluA2-lacking AMPAR antagonist
PHTPP	1μM	ERβ antagonist
Picrotoxin	50μM	$GABA_AR$ antagonist
PPT	25nM, 50nM	ERα agonist
U0126	10μM	ERK inhibitor
Wortmannin	50nM	PI3-Kinase inhibitor